

INTERNATIONAL SOCIETY FOR SOIL MECHANICS AND GEOTECHNICAL ENGINEERING



This paper was downloaded from the Online Library of the International Society for Soil Mechanics and Geotechnical Engineering (ISSMGE). The library is available here:

<https://www.issmge.org/publications/online-library>

This is an open-access database that archives thousands of papers published under the Auspices of the ISSMGE and maintained by the Innovation and Development Committee of ISSMGE.

Causes of Cyclic Shear Failure at Lokanthali of Araniko Highway after Mw7.8 2015 Gorkha Earthquake

Binod Tiwari, Ph.D., P.E.¹ Beena Ajmera, Ph.D.², and Brian Yamashiro³

¹Professor, Civil and Environmental Engineering Department, California State University, Fullerton, 800 N State College Blvd., E-419, Fullerton, CA, 92831.

²Assistant Professor, Civil and Environmental Engineering Department, California State University, Fullerton, 800 N State College Blvd., E-318, Fullerton, CA, 92831.

³Graduate Student, Civil and Environmental Engineering Department, California State University, Fullerton, 800 N State College Blvd., Fullerton, CA, 92831.

ABSTRACT

The M_w 7.8 2015 Gorkha Nepal Earthquake was one among the most devastating earthquakes in the history. It left close to 9,000 people dead, 22,000 people injured and caused over \$5B loss of properties. The earthquake triggered over 15,000 co-seismic landslides. Although the major highways and bridges performed well, majority of the hydropower projects located within the earthquake-affected area sustained different types of damages. A few dozens buildings, including several modern constructions, collapsed in Kathmandu due to the earthquake shaking, killing thousands of people. The earthquake also caused cyclic shear failure of a sector of Araniko Highway at Lokanthali, Kathmandu. This highway is very important trade route to China. A 250 m long stretch of the highway collapsed with vertical movements of more than a meter and lateral displacements of approximately 0.5 m. The landslide seriously damaged dozens of buildings and displaced a few of them by approximately 1 m. To investigate the causes of ground failure, the authors performed site investigation including subsoil exploration, in-situ tests and laboratory tests on the slope forming materials in addition to topographic mapping. Additionally, deformation and limit equilibrium analyses were also performed using the laboratory and field data. The study revealed that earthquake induced shaking in combination with post-cyclic strength degradation of the lacustrine deposit, locally named *Kalimati*, caused the cyclic shear failure although the site has gentle slopes and the earthquake main shock produced relatively moderate ground accelerations at this location.

INTRODUCTION

The $M_w = 7.8$ 2015 Gorkha earthquake was one among the deadliest earthquakes in the South Asian region. It killed close to 9,000 people and injured more than 22,000, displaced millions of residents, and left hundreds of thousands of people homeless. Estimated economic loss resulted due to the earthquake is over \$5B (almost 25% of the Nepalese GDP). The epicenter of the Gorkha earthquake is located at Barpak, Gorkha, approximately 80 km northwest of Kathmandu. The hypocenter of the earthquake is estimated at a shallow depth of 15 km (Hashash et al., 2015). The first author co-lead the NSF funded 15-member GEER team for post-earthquake reconnaissance immediately after the earthquake and spent 30 days in the field to collect perishable geotechnical information. Despite the large magnitude of earthquake, the observed peak ground accelerations, recorded at very few locations in and around Kathmandu valley were relatively small. As such, the damage caused by this earthquake was much less than expected for

an earthquake with this magnitude. However, at clustered locations, significant damage was observed. There was very limited ground motion information that could be useful to analyze and assess the individual damage. One among those limited information was the ground motions (Figure 1) recorded in Kathmandu Valley at the KATNP station, which is located about 6.3 km north-west from the site. USGS released the ground motion data recorded at this station immediately after the earthquake. Both the north-south and east-west components of the peak ground accelerations (PGA) recorded at this station were surprisingly low, at the order of 0.16g. Dixit et al. (2015) analyzed the records from the main shock, as well as additional recordings from aftershocks and microtremors, and reported a dominant period of about 5 seconds for the main shock. Although majority of the highways and bridges performed well during and immediately after the earthquake, several mountain roads including the access roads to hydropower projects were fully damaged at hundreds of locations, completing blocking the through traffic. One among the spectacular damage along the roads in Kathmandu Valley was Lokanthali Cyclic shear failure. This road was widely covered in media and reconnaissance reports. The GEER team mapped the damage, performed open cuts for soil exploration, and performed a few laboratory experiments on the field samples collected during the field visit (Hashash et al. 2015; Moss et al. 2015).

The first author made three more trips to Nepal in addition to the month-long field reconnaissance with the GEER team. The latest trip was in August 2016, to collect post-earthquake field information. Detailed topographic survey, in-situ soil tests, and soil sampling were performed at Lokanthali cyclic shear failure area to evaluate the cause of failure. The subsequent section includes details of those investigation and the results of stability and deformation analyses performed.

EXTENT OF DAMAGE

The 2015 Gorkha Earth caused a significant damage to building structures in Kathmandu and other moderately large towns located in the eastern side of the main shock. Although the level of damage was much less than expected with such large magnitude earthquakes, a few dozen of modern structures were fully or partially damaged, killing hundreds of people (Figure 2). Moreover, majority of the other damaged buildings were constructed with brick masonry structures on mud mortar. Aerial reconnaissance with helicopter revealed that hundreds of buildings located on the ridge of the slopes within the rupture surface were fully collapsed. Dozens of cultural heritage sites and temples were either fully or partially damaged due to the earthquake induced ground shaking.

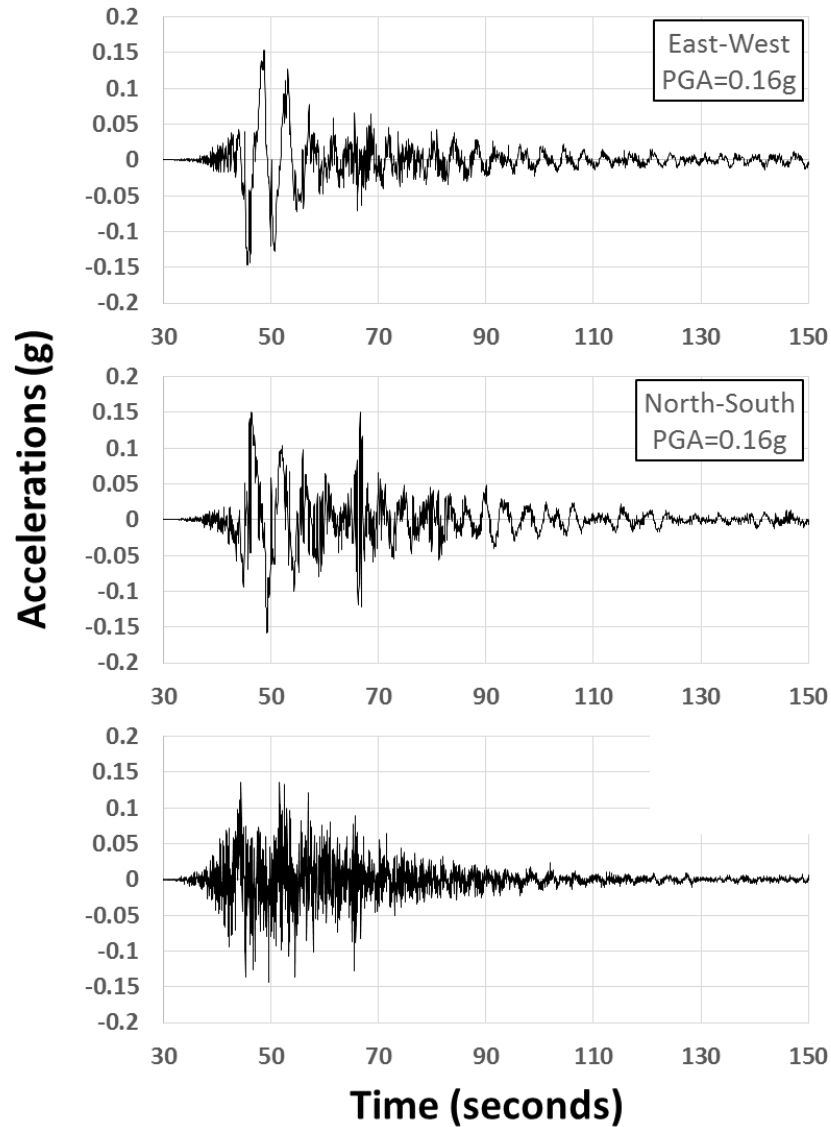


Figure 1. Ground accelerations recorded at the KATNP station during the April 25, 2015 Gorkha earthquake (CESMD, 2015).

The 2015 Gorkha earthquake triggered liquefaction at more than 15 locations (Figure 3). At those locations, traces of liquefied sand ejecta were observed. Some of those ejecta were in significantly large in quantity and the others were clearly visible traces, but not in abundant quantity. The field observation showed that the earthquake shaking was just enough to liquefy the soil, but was not sufficient to cause a massive damage to structures.



Figure 2. Extent of structural damage observed in Kathmandu Valley due to the 2015 Gorkha Earthquake. Majority of the damage were soft-story collapses.

The 2015 Gorkha earthquake significantly affected the hydropower projects. While majority of the damage was observed in the dams, penstocks and powerhouses due to landslides and rock falls, 19 cm of seismically induced settlement was observed on the dam body of the Upper Tamakoshi Hydropower project, the largest Hydropower Project of the nation, which was under construction at the time of earthquake (Figure 4).

As expected, the 2015 Gorkha earthquake triggered approximately 15,000 co-seismic landslides (Figure 5). Approximately 3,500 of these landslides were larger than 100 m² in area. Tiwari et al. (2016) correlated those landslides with terrain slope, geology, and peak ground acceleration (PGA) and reported that slope inclination and PGA were the most influencing factor in triggering those landslides. More than 99% of those triggered landslides were disruptive landslides. Although very small in number, the coherent landslides triggered by the earthquake caused significant damage to structures and killed hundreds of people. Two among those landslides are Langtang Debris Avalanche and Lokanthali cyclic shear failure. Description of Langtang Debris Anavalche and other valley blocking landslides are available in Hashash et al. (2015), Moss et al. (2015) and Collins and Jibson (2015). This article discusses in detail about the Lokanthali cyclic shear failure site.



Figure 3. Sand ejecta observed at the edges of Kathmandu Valley due to liquefaction. The liquefaction sites, although were wide spread, did not damage structures.



Figure 4. 19 cm settlement observed at the main dam of Upper Tamakoshi Hydropower project due to seismically induced settlement of the foundation material.

Lokanthali cyclic failure site is located about 1 km east of Kathmandu airport in Nepal ($27^{\circ}40'28.1''N$, $85^{\circ}21'44.6''E$). Hashash et al. (2015) and Moss et al. (2015) mapped this failure site. Field evidence of ground failure was observed along a ridge for a distance of about 1 km. At different locations, fissures larger than 2 m and tension cracks with vertical offsets larger than 1.4 m along the top of the ridge, were observed (Figure 6). The surprising feature of this cyclic failure was that the ground slope was very gentle and such failure was not expected at this newly renovated highway.



Figure 5. Typical co-seismic landslides observed in various parts of the country due to the 2015 Gorkha Earthquake.

The authors conducted post-earthquake field investigation to evaluate the damage condition and potential cause of ground failure. The cyclic failure caused three major types of damage – a) partial collapse and major settlement of approximately 250 m length of Araniko Highway (Figure 7), b) partial or complete damage of many modern structures (Figure 8), c) development of tension cracks and settlement at 300 m x 300 m plan area (Figure 9).

Major portion of the settled highway is presented in Figure 7. This portion of the highway was constructed during the recent road improvement and includes an engineered fill within MSE walls (that can be seen in Figure 9). Figure 9 shows a few cracks observed along the eastern and western boundaries of the landslide. More than 1 m of vertical drop was observed at different locations within the residual area in the southeastern side of the distressed highway. Several buildings, located in the unstable side of the slope, were observed to have moved by 0.5-1.0 m along with their foundations without having a noticeable tilt in the building. Settlement occurred on both east and west sides of the highway ends near the creek, presented in Figure 10. This creek, which accumulates a large amount of surface run-off during the rainy season (that the authors observed during their field investigation during mid-monsoon period), is currently channelized with approximately 60 cm. diameter concrete pipes.



Figure 6. Observed main distress features at Lokanthali site and locations of in-situ investigation performed for this study (indicated by points “B”).



Figure 7. Overall view of distressed portion of Araniko Highway at Lokanthali, Left: North side of the highway; Right: South side of the highway.

INVESTIGATION AND SHEAR TESTING

The Kathmandu valley was formed during the Pliocene to Pliostecene geologic eras by draining the lake water from an outlet point (Yoshida and Gautam, 1988). The subsurface materials in the Kathmandu valley consist mainly of deep lacustrine deposits, which locally are on the order of 600 m thick (Piya 2004). River incisions and excavation activities for different purposes such as highway and building construction locally expose these lacustrine deposits throughout the valley.

Where observed, the deposits consist mainly of poorly consolidated plastic clays and silts, locally interlaid by thin sandy layers.



Figure 8. Typical structural damage observed during the field investigation.

Tiwari and Pradel (2016) conducted field investigation of the study area in August 2015. They explored the subsurface conditions at six locations in the vicinity of Araniko Highway, in the area where seismic ground movements were most prevalent (Figure 6). The most prevalent material at Lokanthali, was a dark grey to black plastic clay, locally known as “Kalimati”, i.e., “black cotton clay” (Figure 11). Later, the authors of this article collected soil samples from the study area and conducted various soil tests at California State University Fullerton. Based on the laboratory test results, the natural moisture content, fine content, clay fraction, liquid limit, plasticity index, and USCS classification of these soft clays were 30-36%, 80-85%, 10-26%, 32-46, 12-17, and ML, respectively. The x-ray diffraction of the separated clay fraction from the soil collected showed dominance of illite with significant proportions of kaolinite.

To assess the strength of this material, Tiwari and Pradel (2016) conducted Swedish Cone Tests (SCT, also commonly known as the Swedish Weight Sounding tests), and in-situ Vane Shear Tests (VST). The undrained shear strengths obtained from both VST and SCT tests are available in Tiwari and Pradel (2016). The effects of near surface desiccation were apparent near ground surface. However, below a depth of 2.5 m, the clays at Lokanthali generally became saturated and were found to be extremely soft. The VST residual strength tests showed that Kalimati clay has high sensitivity. Hence, that its strength is expected to drop rapidly and significantly during cyclic shearing.



Figure 9. Left: Observed tension cracks and settlements throughout the study area.



Figure 10. Concrete pipe and open culvert that used to drain the water from the study area.



Figure 11 (Left). Left: Typical soil profile observed near the main scarp location; Center: Lacustrine deposits exposed along road cut (27°40'30.6"N, 85°21'42.4"E), composed of plastic clay beds separated by very thin sand layers (light grey in the photo); Right: Type of material observed during subsoil exploration.

DYNAMIC STRENGTH PROPERTIES OF SOIL FROM LOKANTHALI SITE

Soil samples were collected from BH 2 of the study area (Figure 6) from four different depths ranging from 0.5 m to 3.0 m. The soil samples were reconstituted at the liquidity index of 1 and consolidated in a constant volume simple shear device at effective normal stresses ranging from 25 to 800 kPa to measure undrained shear strength and corresponding fully softened shear strengths. The laboratory shear test results (Figure 12) shows the undrained strength ratios of 0.25 to 0.47. The fully softened shear strength was obtained from the effective stress analysis of the constant volume direct simple shear device, as presented in Figure 12. The secant fully softened friction angles ranged from 21.5° to 37.5°.

Soil samples collected from the study area was reconstituted at liquidity index of 1 and consolidated in cyclic simple shear device and cyclically sheared at different cyclic stress ratios (CSRs) until 2.5%, 5%, and 10% double amplitude shear strains were observed. The methodology for the cyclic shear tests are similar to that explained in Ajmera et al. (2015). Shown in Figure 13 are the cyclic strength curve and backbone curve of Lokanthali Soil Sample No. 1. Likewise, G/G_{max} as well as damping ratio vs shear strain plots are presented in Figure 14. Considering the CSRs of the tested soil, the CSRs of the soil for 5% double amplitude strain is about 0.15 only. Likewise, the test results show that the soil significantly drop its stiffness with an increase in shear strain. Moreover, the soil exhibit over 50% damping at 1% shear strain. The result of monotonic simple shear test immediately after the cyclic loading showed a post-cyclic strength degradation of 71%. This amount of reduction is close to the reduction amount proposed by Ajmera et al. (2015), as shown in Figure 15.

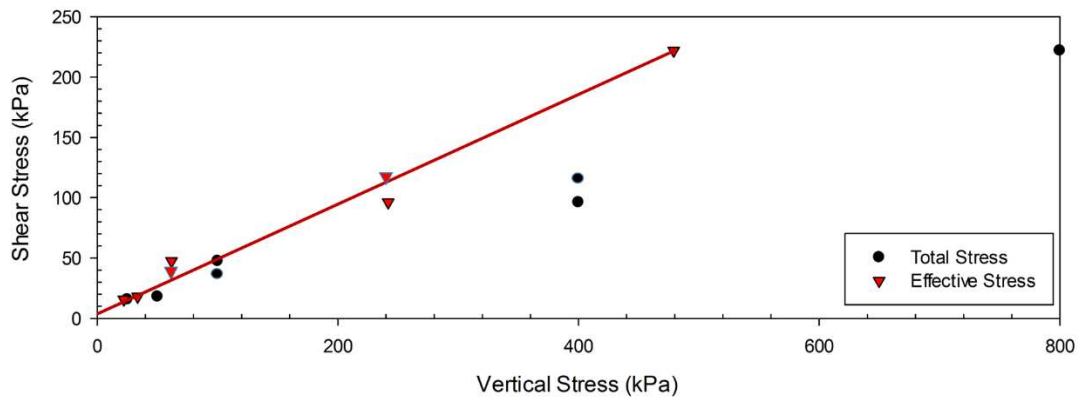


Figure 12. Total and effective shear envelopes obtained from the constant volume monotonic direct simple shear tests for Lokanthali soil Sample 1.

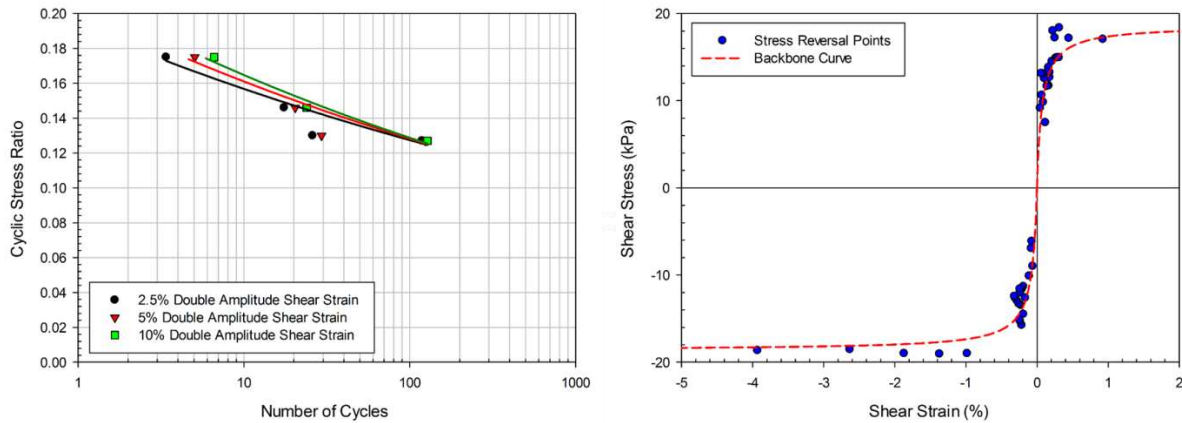


Figure 13. Cyclic stress curves and backbone curves for Lokanthali soil Sample 1.

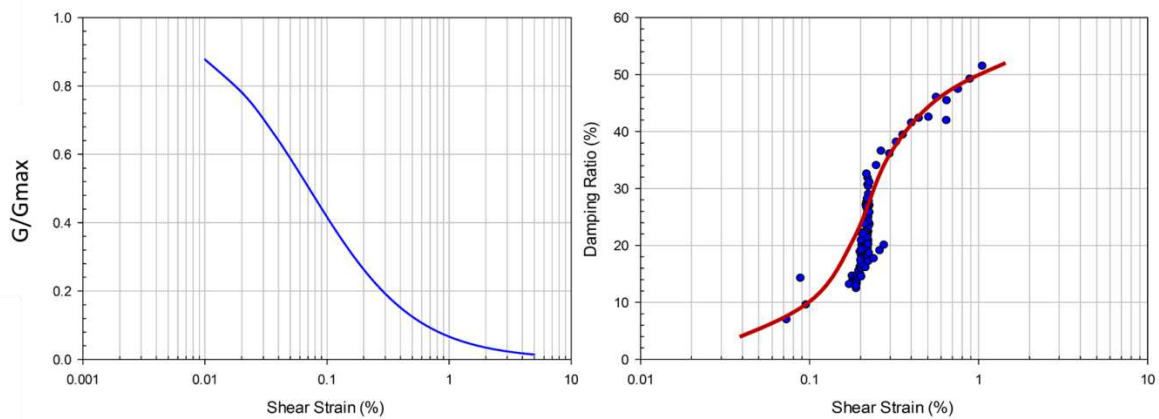


Figure 14. G/G_{max} and damping curves for Lokanthali soil Sample 1.

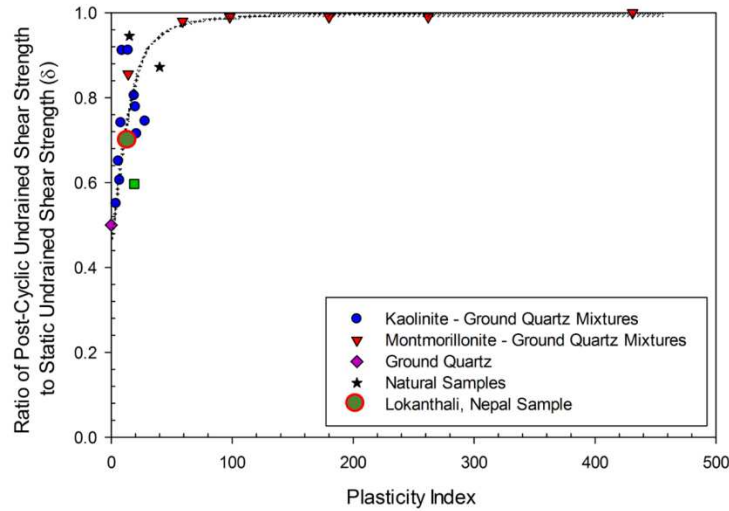


Figure 15. Post-cyclic strength degradation for Lokanthali soil Sample 1, plotted in the strength degradation chart proposed by Ajmera et al. (2015).

DEFORMATION ANALYSIS RESULTS AND POSTULATED FAILURE MECHANISMS

Considering the clays to be very soft and having very small undrained strength ratios depicted both by the laboratory tests and the in-situ measurements, the slope failure at Lokanthali can be considered as a result of seismic activities. Based on the plasticity indices of the materials obtained from the laboratory tests, liquefaction is not considered to be the cause of failure. However, the strongest possible cause of failure could be the reduction in undrained shear strength in combination of seismic force induced by the earthquake. The authors conducted deformation analyses using Phase²v8 (RocScience, 2016) for the cross-section geometry of the Lokanthali ground profile (that was obtained from the field investigation) and the undrained shear strength parameters obtained from the laboratory tests and the strong motion data recorded at the KATNP station, which is close to the study area.

Results of the deformation analyses after the earthquake without and with strength degradation are presented in Figures 16 and 17, respectively. As can be observed from Figure 16, the slope was stable prior to the earthquake and after the earthquake considering the shear strength of soil prior to earthquake. When a strength degradation of 70% (which was obtained from the laboratory test) was applied, maximum horizontal displacements of approximately 1.2 m was observed. Magnitude and amount of those deformations are close to that observed in the field. When the ground motion after the major aftershock of Mw7.3 was applied, the slope did not show any additional deformation. The first author was at Lokanthali site at the time of the Mw 7.3 earthquake and confirmed that the earthquake did not trigger any further movements of the slope. The numerical study result shows that the shear strength degradation in combination with the seismic loading were responsible for the cyclic shear failure at Lokanthali.

Tiwari and Pradel (2016) performed non-linear dynamic geomechanical numerical analyses using deconvoluted ground motions from the recordings at KATNP using the lower and upper bound strengths obtained from in-situ tests. They performed numerical analyses using the

computer program FLAC version 7.0 (Itasca, 2011). Their numerical analysis result shows the the vertical and horizontal displacements of 1.0 m and 0.5 m, respectively, which is close to the results obtained from this study.

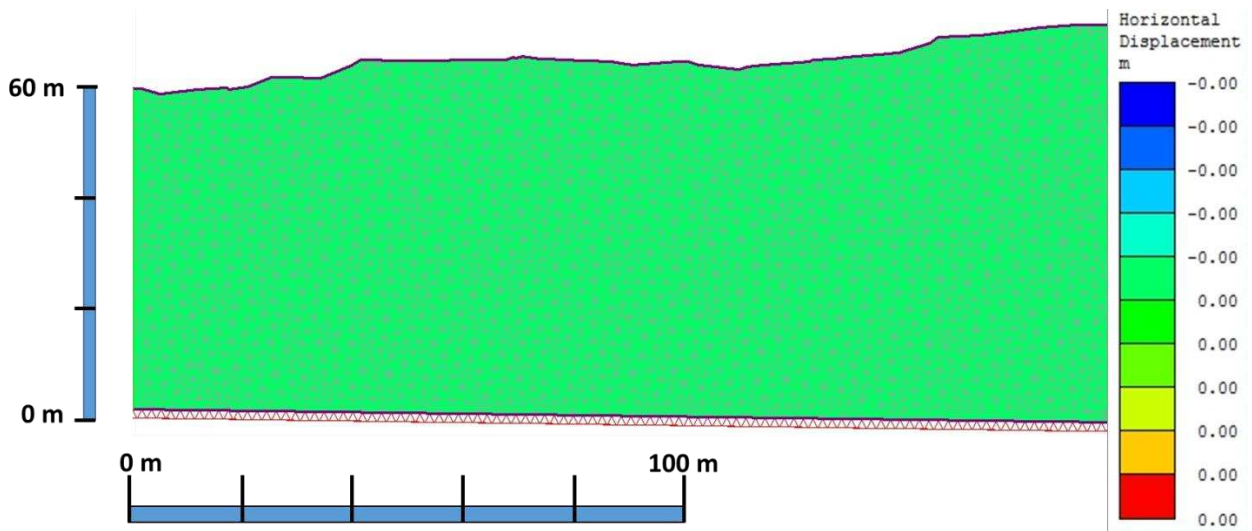


Figure 16. Horizontal displacement of slope obtained after earthquake load without strength degradation, as calculated from numerical analysis

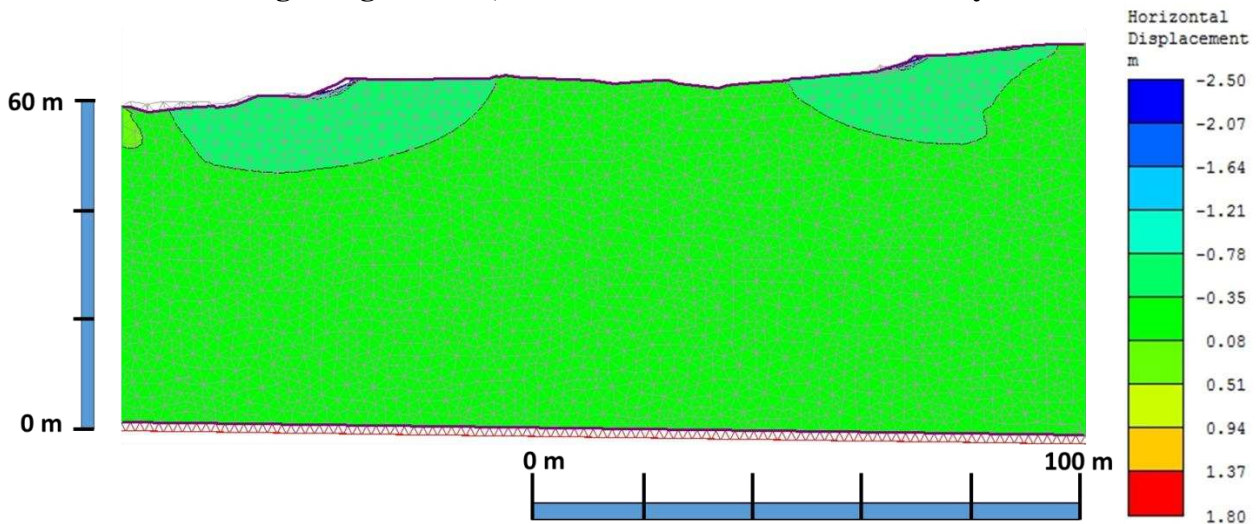


Figure 17. Horizontal displacement of slope obtained after earthquake load with strength degradation, as calculated from numerical analysis

CONCLUSION

Lokanthali cyclic shear failure was one among the major geotechnical damages caused by the 2015 Gorkha Earthquake. In-situ Vane Shear and Swedish Cone Tests conducted on the site revealed that the site is underlain by very soft, plastic lacustrine clays that have very low shear strength and high sensitivity, which are highly vulnerable to seismically induced sliding. The laboratory test results conducted on the soil collected from the site revealed post-cyclic strength degradations of 70%. The numerical analyses conducted by the authors show that the cyclic

failure would not occur with earthquake induced ground motion if the shear strength would not have degraded after the earthquake shaking. The horizontal and vertical displacements obtained from the numerical analyses were consistent observed values in the field. Thus Lokanthali cyclic shear failure is attributed to combination of the cyclic loading and associated shear strength degradation.

REFERENCES

- Ajmera, B., Brandon, T., and Tiwari, B. (2015). "Cyclic Strength of Clay-Like Materials," Proceedings of 6th International Conference on Earthquake Geotechnical Engineering, Christchurch, New Zealand.
- ASTM (2008), "Standard test method for field vane shear test in cohesive soil. ASTM standard D2573-08", ASTM International, West Conshohocken, Penn.
- CESMD (2015), "Center for Engineering Strong Motion Data record of USGS Station KATNP on April 25, 2015.
- Collins B.D. and Jibson R.W. (2015), "Assessment of Existing and Potential Landslide Hazards Resulting from the April 25, 2015 Gorkha, Nepal Earthquake Sequence", USGS Open-File Report 2015-1142.
- Dixit A.M. et al. (2015), "Strong-motion observations of the M 7.8 Gorkha, Nepal, earthquake sequence and development of the N-SHAKE strong-motion network." Seismological Research Letters 86.6 1533-1539.
- ENV 1997:3-2000, (2000), Euro Code 7: Geotechnical Design Assisted by Field Testing, 146.
- GEER (2015) "Geotechnical Field Reconnaissance: Gorkha (Nepal) Earthquake of April 25 2015 and Related Shaking Sequence", Geotechnical Extreme Event Recon. Report No. GEER-040.
- Itasca (2011), "FLAC (Fast Lagrangian Analysis of Continua) Version 7.0," Minneapolis, USA, www.itascacg.com.
- JGS (2004), Japanese Standards for Geotechnical and Geoenvironmental Investigation Methods, Standards and Explanations (in Japanese), p.125.
- Moss, R. et al. (2015). Geotechnical Effects of the 2015 Magnitude 7.8 Gorkha, Nepal Earthquake and Aftershocks, Seismological Research Letters, 86, 1514-1523.
- Piya (2004), "Generation of a geological database for the liquefaction hazard assessment I Kathmandu Valley, Natural Hazard Studies, Enschede, The Netherlands, ITC.
- RocScience (2016), "Phase² v8"
- Seed H.B. and Idriss I.M. (1970), "Soil Moduli and Damping Factors for Dynamic Response Analyses," Report No. UCB/EERC 70/10, Earthquake Engineering Research Center, University of California, Berkeley.
- Tiwari, B., Ajmera, B., Dhital, S., and Sitoula, N. R. "Geological, Topographical and Seismological Control on the Co-Seismic Landslides Triggered by the 2015 Gorkha Earthquake," Geotechnical Special Publication 2017 (In Press).
- Tiwari B. and Pradel D. (2016) "CASE STUDY: Landslide Movement at Lokanthali during the Mw = 7.8 Gorkha (Nepal) Earthquake of April 25 2015", Geotechnical Special Publication, ASCE Press, in press.
- Yoshida M. and Gautam P. (1988), "Magnetostratigraphy of Plio-Pleistocene lacustrine deposits in the Kathmandu Valley, central Nepal." Proceedings of Indian National Science Academy A 54 (1988): 410-417.